WIND ENERGY
Wind Energ. 2015; **00**:1–16
DOI: 10.1002/we

RESEARCH ARTICLE

Testing and validation of multi-lidar scanning strategies for wind energy applications

Jennifer F. Newman[1,*], Timothy A. Bonin[1,+], Petra M. Klein[1], Sonia Wharton[2], Rob K. Newsom[3]

[1]School of Meteorology, University of Oklahoma, Norman, OK, USA
[2]Atmospheric, Earth and Energy Division, Lawrence Livermore National Laboratory, Livermore, CA, USA
[3]Pacific Northwest National Laboratory, Richland, WA, USA
*Current affiliation: National Wind Technology Center, National Renewable Energy Laboratory, Golden, CO, USA
+Current affiliation: Cooperative Institute for Research in the Environmental Sciences, University of Colorado, and National Oceanic and Atmospheric Administration/Earth System Research Laboratory, Boulder, CO, USA

ABSTRACT

Several factors cause lidars to measure different values of turbulence than an anemometer on a tower, including volume averaging, instrument noise, and the use of a scanning circle to estimate the wind field. One way to avoid the use of a scanning circle is to deploy multiple scanning lidars and point them toward the same volume in space to collect velocity measurements and extract high-resolution turbulence information. This paper explores the use of two multi-lidar scanning strategies, the tri-Doppler technique and the virtual tower technique, for measuring 3-D turbulence.

In Summer 2013, a vertically profiling Leosphere WindCube lidar and three Halo Photonics Streamline lidars were operated at the Southern Great Plains Atmospheric Radiation Measurement site to test these multi-lidar scanning strategies. During the first half of the field campaign, all three scanning lidars were pointed at approximately the same point in space and a tri-Doppler analysis was completed to calculate the three-dimensional wind vector every second. Next, all three scanning lidars were used to build a "virtual tower" above the WindCube lidar.

Results indicate that the tri-Doppler technique measures higher values of horizontal turbulence than the WindCube lidar under stable atmospheric conditions, reduces variance contamination under unstable conditions, and can measure high-resolution profiles of mean wind speed and direction. The virtual tower technique provides adequate turbulence information under stable conditions but cannot capture the full temporal variability of turbulence experienced under unstable conditions because of the time needed to readjust the scans.

KEYWORDS

Doppler lidar, turbulence, virtual tower, scanning lidar

Correspondence

National Wind Technology Center, National Renewable Energy Laboratory, 15013 Denver West Parkway, Golden, CO
E-mail: Jennifer.Newman@nrel.gov

Received . . .

1. INTRODUCTION

An accurate wind resource assessment requires an estimate of wind speeds and turbulence across the heights spanned by a turbine rotor disk (typically 40 to 120 m above ground level; AGL; [1]). Traditionally, these measurements have been made with cup anemometers on tall meteorological towers. However, as turbine hub heights extend further into the atmosphere, it has become more difficult and costly to build tall towers that reach these heights. In response to this issue, the use of remote sensing devices has recently emerged as an alternative to tall towers and remote sensing instruments are now commonly employed in wind-energy studies.

One frequently used remote-sensing instrument is a Doppler lidar (light detection and ranging), which utilizes the Doppler shift of backscattered laser energy to estimate the wind speed within a volume of air. Two of the most commonly used lidar scanning strategies are the Doppler beam-swinging (DBS; [2]) strategy and the velocity azimuth display (VAD;

[3]) strategy. Both of these strategies involve directing the laser beam to different points around a scanning circle and using geometrical considerations to estimate the mean wind speed and direction. A major assumption in these techniques is that the mean flow is horizontally homogeneous throughout the scanning circle, which is often invalid in complex terrain (e.g., [4]), within wind turbine wakes [5] and under convective conditions [6], causing errors in lidar-measured wind speeds. The DBS and VAD techniques can also cause errors in the measurement of turbulent quantities. Combining data from different beam positions in these scans results in variance contamination, where extra variance components contaminate the true value of the variance [7].

One way to avoid the use of a scanning circle is to steer the lidar beam to a particular point in space. In this way, the line-of-site velocity and velocity variance can be estimated without potential errors from variance contamination and horizontal heterogeneity. If one or two additional lidars are pointed toward this volume of air, a two- or three-dimensional velocity vector can be derived (e.g., [8, 9]). However, the use of multiple lidars to measure turbulence is still a relatively new concept, and it is unclear if turbulence information can be accurately provided by multi-lidar scanning strategies. Research-grade scanning lidars, while prohibitively expensive, are generally required for the implementation of multi-lidar scanning strategies. Thus, multi-lidar scanning strategies must provide valuable mean wind speed and turbulence information for wind farm operators in order to offset the cost of purchasing or renting the scanning lidars.

To evaluate the ability of multi-lidar scanning strategies to measure wind speeds and 3-D turbulence, three scanning lidars and a vertically profiling WindCube lidar were operated during the summer of 2013 at the Southern Great Plains Atmospheric Radiation Measurement (ARM) site, a field measurement site located in northern Oklahoma and instrumented with various in-situ and remote sensing devices. This work marks the first time the tri-Doppler and virtual tower techniques have been evaluated under vastly different stability conditions at the same site and compared to measurements from a commercially available lidar. The evaluation of both techniques at the same site allows for the comparison of the techniques under similar atmospheric conditions while utilizing the same scanning lidars for both techniques. Comparisons to data obtained from a commercially available lidar are extremely valuable, as they directly indicate any advantage of using a multi-lidar scanning technique as opposed to a single commercially available lidar.

2. BACKGROUND

Initially, multi-lidar research focused on the use of two Doppler lidars to measure horizontal wind speeds and turbulence structures. Calhoun et al. [10, 11] were one of the first to discuss a technique for implementing multi-Doppler lidar scans and extracting 2-D velocity information from the resulting data. With a focus on measuring mean wind speed profiles in an urban area for dispersion model verification, Calhoun et al. [11] used two Lockheed Martin WindTracer Doppler lidars during the Joint Urban 2003 experiment in Oklahoma City. The lidars performed a series of overlapping range-height indicator (RHI) scans to measure the horizontal wind speed, creating several "virtual towers" in the downtown Oklahoma City area.

The increasing commercial availability of research-grade scanning lidars has made it possible to conduct more extensive multi-lidar scanning campaigns. Newsom et al. [12] deployed two scanning Halo Streamline lidars at the Southern Great Plains ARM site to conduct dual-Doppler scans. Newsom et al. [12] found that one-minute dual-Doppler retrievals of wind speed were well-correlated with measurements from a 3-D sonic anemometer, radar wind profiler, and radiosonde from the site. Fuertes et al. [13] used three Halo Streamline lidars at the Experimental Site for Atmospheric Research in Cabauw, The Netherlands to conduct a tri-Doppler scan technique. Fuertes et al. [13] used spatial and temporal filters to approximate the wind speed that would be measured by 3-D sonic anemometers on the measurement site tower if they were subject to the same temporal resolution and volume averaging constraints as the Streamline lidars. Turbulence statistics determined from the tri-Doppler technique and the filtered sonic data compared favorably at a height of 60 m AGL.

The presented work also uses three Halo Streamline scanning lidars to conduct a series of tri-Doppler scans. However, while past research has only focused on either the virtual tower technique (e.g., [11, 12]) or a tri-Doppler stare scan (e.g., [9, 13]), the presented work provides an evaluation of both techniques at the same measurement site during back-to-back time periods. Results from this experiment will show the advantages and disadvantages of using multi-lidar scanning strategies for wind energy turbulence measurements under different atmospheric stability conditions. Recommendations are also made for avenues of future research for the evaluation of multi-lidar scanning strategies.

3. EXPERIMENTAL OVERVIEW

The multi-lidar field experiment took place as part of the Lower Atmospheric Boundary Layer Experiment (LABLE) at the Southern Great Plains ARM site near Lamont, Oklahoma. LABLE took part in two phases: LABLE 1 was conducted from 18 September to 13 November 2012 and LABLE 2 was conducted from 12 June to 3 July 2013. While LABLE 1 focused on comparisons between different remote sensing and in-situ instruments, LABLE 2 is presented here for the first

Wind Energ. 2015; **00**:1–16 © 2015 John Wiley & Sons, Ltd.
DOI: 10.1002/we
Prepared using weauth.cls

time in detail and focused on the evaluation of different lidar scanning strategies for turbulence measurements. Further information on the instrumentation and research goals of LABLE can be found in Klein et al. [14] and an examination of nocturnal boundary layers experienced during LABLE 1 can be found in Bonin et al. [15].

3.1. Southern Great Plains ARM Site

The ARM site is situated in flat, fairly uniform terrain in an area of Oklahoma with high wind resource potential; in fact, a large operational wind farm is located in the same area. Fig. 1 shows the location of the ARM site in northern Oklahoma, in addition to the terrain surrounding the ARM central facility.

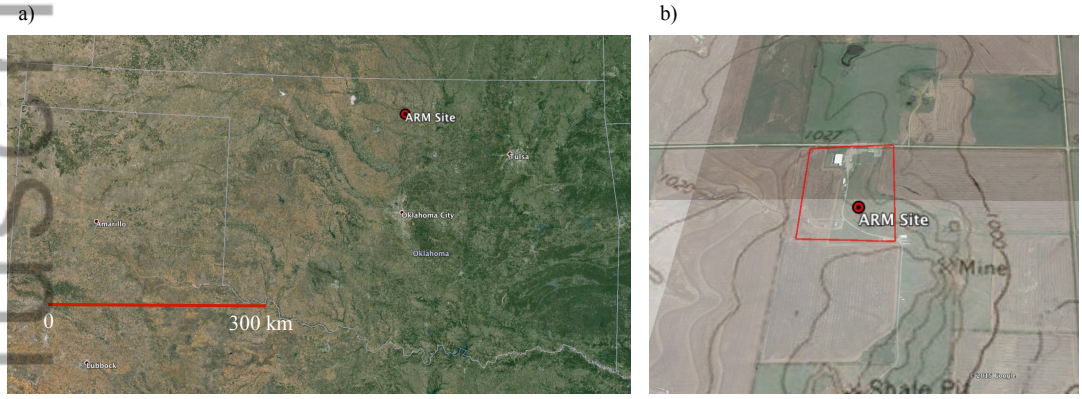

Figure 1. a) Google Earth image of the state of Oklahoma. Location of Southern Great Plains ARM site is denoted by red marker. b) Google Earth image of the central facility of the Southern Great Plains ARM site (outlined in red box) with overlaid elevation contours in feet. Elevation map is from the United States Geological Survey and with contour intervals of approximately 10 feet (3.05 m).

Locations of the various instruments used in LABLE 2 are shown in Fig. 2. The OU Streamline is the scanning lidar owned by the University of Oklahoma (OU), and the ARM Streamline is the scanning lidar permanently located at the ARM site. The Galion lidar was rented from Sgurr Energy by Lawrence Livermore National Laboratory (LLNL) and has identical hardware to the two Streamline lidars. The WindCube lidar is a commercially available vertically profiling lidar owned by LLNL.

3.2. Instrumentation

The three scanning lidars (OU Streamline, ARM Streamline, and Galion) are pulsed heterodyne lidars equipped with a scanner that can move in both azimuth and elevation. Because the position of the lidar beam can be easily changed, the scanning lidars can conduct both RHI and plan-position indicator (PPI) scans, as well as specialized scans programmed by the user. In contrast, the WindCube lidar uses a rotating prism to steer the lidar beam in azimuth and is limited to scanning at a fixed elevation angle of 62°. Technical specifications and configurations of the lidars are summarized in Table I. Detailed information for the Halo Photonics system can be found in Pearson et al. [16].

Data from a 60-m meteorological tower were also available during the experiment. Gill Windmaster Pro 3-D sonic anemometers are mounted on the tower at 25 and 60 m. A 4-m flux tower is also located near the base of the 60-m tower and collects surface meteorological data in addition to sonic anemometer data. More information can be found in the ARM instrument handbook [17]. Sonic anemometer data were collected at a frequency of 10 Hz.

As the 60-m sonic anemometer frequently experienced data outages during the experiment, only data from the 4- and 25-m sonics are shown in this work. Data at these heights are shown to depict the wind field below the minimum measurement height of the lidars.

3.3. Lidar Scanning Strategies

3.3.1. WindCube Scanning Strategy

The WindCube v2 lidar measures wind speed with a DBS technique [2], where the lidar beam is pointed in the four cardinal directions (north, east, south, and west), then pointed vertically, and the wind components are determined

Lidar Configurations		
	Leosphere WindCube v2	**Halo Photonics Streamline**
Wavelength	1.5 μm	1.5 μm
Min. Range	40 m	105 m
Max. Range	200 m	9.6 km (4 km for Galion)
Range Resolution	20 m	30 m
Sampling Rate	1 Hz	1 Hz
Scanning Azimuth Angles	0, 90, 180, 270°	User-defined: 0–360°
Scanning Elevation Angles	62, 90°	User-defined: 0–90°

Table I. Technical specifications and configurations for lidars used in LABLE 2. Unless otherwise noted, specifications for Galion lidar are identical to those listed for Streamline lidar. Azimuth angles are measured from true north and elevation angles are measured from ground level.

from geometrical considerations. This process takes just under one second per beam location, such that a full DBS scan is completed approximately every four seconds. However, the WindCube velocity algorithm calculates the velocity components every second using the current radial velocity and the radial velocities obtained from the previous four beam locations [18]. The time series of these velocity components (u, v, and w) can then be used to estimate turbulence parameters including the three variance components (σ_u^2, σ_v^2, and σ_w^2). The vertical variance, σ_w^2, can be measured in two different ways: by calculating the variance of the DBS-estimated vertical velocity component or by calculating the variance of the radial wind speed measured by the vertically pointing beam position.

Several major problems arise when using the DBS technique to measure turbulence [e.g., 7, 19]. Errors due to volume averaging are inherent in remote sensing technology for any kind of scanning strategy; the velocity measured by a lidar is the weighted average of all aerosol velocities within the probe volume. Thus, turbulence scales that are smaller than the probe volume cannot be measured accurately. The particular scanning strategy used by the WindCube lidar, the DBS technique, also induces errors in the turbulent components. When data from all four off-vertical beams are combined to estimate the turbulent components, it is assumed that the instantaneous velocity components are the same at opposite ends of the scanning circle. However, this assumption is generally not true in turbulent flow, when the values of the instantaneous velocity components change rapidly in time and space. Changes in the instantaneous velocity values across the scanning circle result in additional variance components that contaminate the true value of the variance [7]. While volume averaging decreases the value of the lidar-estimated variance, variance contamination increases the variance [7].

3.3.2. Tri-Doppler Technique

In the first multi-lidar scanning strategy, two of the scanning lidars (OU Streamline and Galion) were pointed 105 m above the ARM Streamline lidar, which corresponds to the first useable range gate of the Streamline lidars. While the ARM Streamline lidar pointed directly upward to obtain a direct measurement of the vertical velocity, the OU Streamline and Galion lidars obtained measurements of the radial velocity along their line of sight (Fig. 2a).

To calculate the velocity components, the radial velocity measured by each lidar, $v_{r,lidar}$ (m s^{-1}), is written as the dot product between the true three-dimensional velocity vector, $\mathbf{U}$ (m s^{-1}), and the unit vector of the lidar system, $\mathbf{r_{lidar}}$ (unitless), as in [11]:

$$\begin{aligned} v_{r,lidar} &= \mathbf{r_{lidar}} \cdot \mathbf{U} \\ &= u\cos(\phi)\sin(\theta) + v\cos(\phi)\cos(\theta) \\ &+ w\sin(\phi), \end{aligned} \tag{1}$$

where ϕ and θ are the elevation and azimuthal angles of the lidar beam, respectively. Because the temporal resolution of all three scanning lidars is approximately 1 Hz, the three-dimensional velocity vector at 105 m was also estimated at a frequency of 1 Hz.

Data from the tri-Doppler technique can also be used to estimate mean wind speed profiles. The radial velocity data measured by the OU Streamline and Galion lidars at different ranges, indicated by the markers in Fig. 2a, can be combined using a dual-Doppler technique to calculate a mean horizontal wind speed profile, with the assumption that $\overline{w} \approx 0$ m s^{-1}.

Wind Energ. 2015; **00**:1–16 © 2015 John Wiley & Sons, Ltd.
DOI: 10.1002/we
Prepared using weauth.cls

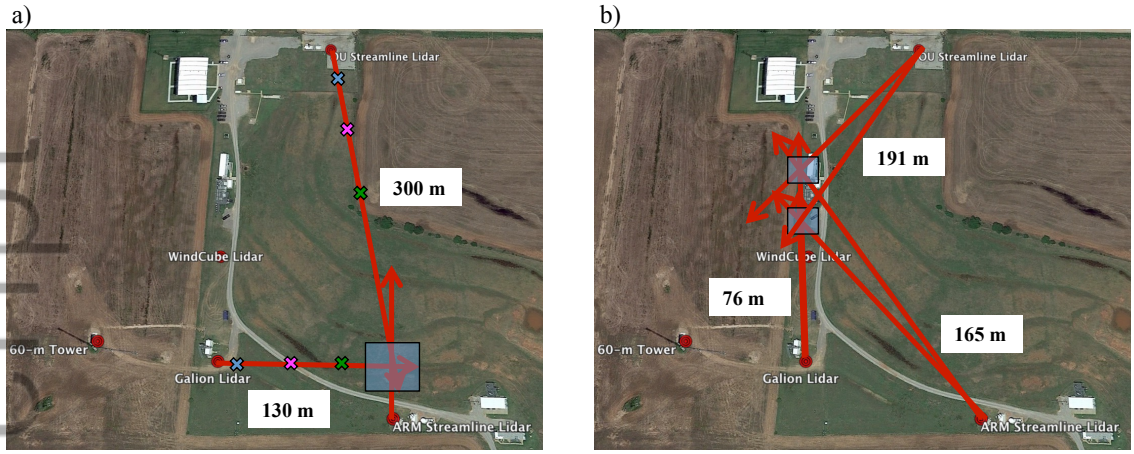

Figure 2. Schematic of the a) tri-Doppler technique and b) virtual tower technique tested during the experiment. Approximate pointing angles of lidars are indicated by red lines with arrows and sample analysis areas are highlighted by blue boxes. Distances between lidars are indicated in white boxes. Colored symbols in a) along OU Streamline and Galion lidar beams illustrate matching measurement heights used to calculate wind profiles with the dual-Doppler technique.

3.3.3. Virtual Tower Technique

The second multi-lidar scanning strategy involved the use of all three scanning lidars to build a "virtual tower" over the WindCube lidar (Fig. 2b). This strategy was identical to the tri-Doppler technique, except the beams were moved to different heights AGL every 10 min. The sampled heights were 60, 100, 200, 350, and 500 m.

Ideally, the beams of the scanning lidars would be rapidly moved from one height to another so that velocity measurements with high temporal resolution could be obtained at all measurement heights. However, although the scanning lidars only collect measurements for one second, it takes several additional seconds to move the lidar beam to a different position and begin collecting measurements again. Thus, a 10-min stare period was selected for each height to ensure that all three scanning lidars had time to adjust to the new measurement height and start collecting measurements. Additionally, although each full virtual tower scan took 60 min, the software installed on all three of the scanning lidars did not restart each scan immediately and instead calculated an approximate scan time for a complete virtual tower scan and then waited until this full time had elapsed before restarting the scan. Thus, the 10-min periods of measurements at each height were actually taken approximately 1.75 hours apart. It is likely that this issue with the scanning software will not be present in later versions, leading to faster virtual tower scan times.

4. DATA PROCESSING

4.1. Time and Location Synchronization

Multi-lidar scanning strategies require that the scanning lidars are synchronized in time and that the exact locations of the lidars are known [11]. The lidars must be scanning the same volume of air at the same time in order to accurately combine the lidar data in velocity variance calculations.

The computer clocks of the various lidars were examined at the start of the experiment and small, consistent differences were noted among the lidar timestamps. During post-processing, timestamps of the different lidars were corrected and radial velocity data from the lidars were interpolated to a one-second grid using a linear interpolation.

Lidar alignment was verified following the technique of Calhoun et al. [11]. At the start of the experiment, the OU Streamline and Galion lidars conducted short PPI scans at low elevation angles in the direction of the tower until the tower appeared as a hard target on the lidar display. The azimuthal angle at which the tower appeared was recorded and compared to the expected azimuthal angle calculated from Google Earth. The difference between these two angles was then used to adjust the bearing of the lidars such that true north corresponded to the 0° azimuthal angle. A similar technique was used once per day to verify the alignment of the ARM Streamline lidar.

4.2. Coordinate Rotation

Before the variance was calculated, a coordinate rotation was applied to the lidar and sonic anemometer data. Following the procedure outlined by Kaimal and Finnigan [20], the data were first rotated such that the mean meridional wind speed, $\overline{v}$, was set to zero. Next, the coordinate axes were rotated such that $\overline{u}$ was aligned with the mean wind direction and $\overline{w}$ was forced to zero.

4.3. Stability Classification

Due to unexpected maintenance on the 60-m tower during LABLE 2, sonic anemometer data coverage was poor and data were often not available to calculate stability parameters. In addition, the quality of temperature and mean wind speed data from the sonic anemometers was questionable during LABLE 2. Thus, data from outside the ARM site were used to calculate stability parameters during the experiment. The Oklahoma Mesonet, a series of over 100 surface meteorological stations, is operated across the state of Oklahoma by OU and Oklahoma State University and was operational during LABLE 2. Mesonet sites record air temperature at 1.5 and 9 m AGL and wind speed at 2 and 10 m AGL every five minutes [21]. The availability of temperature and wind speed data at two different levels allows for the calculation of the gradient Richardson number, *Ri*.

Ri can be approximated by the following equation [22, 23]:

$$Ri = \frac{g[(T_{z2} - T_{z1})/\Delta z_T + \Gamma_d]\Delta z_U^2}{T_{z1}(U_{z2} - U_{z1})^2} \tag{2}$$

where g (m s^{-2}) is the gravitational acceleration, T (K) is the temperature, U (m s^{-1}) is the mean horizontal wind speed, Γ_d (K m^{-1}) is the dry adiabatic lapse rate, $z1$ and $z2$ (m) correspond to the measurement heights for temperature and wind speed, and Δz_T and Δz_U (m) refer to the differences in measurement levels for T and U. The Blackwell Mesonet site is located just over 25 km northeast of the ARM site. *Ri* values calculated from the Blackwell Mesonet site and from the limited tower data at the ARM site corresponded to approximately the same stability classifications during the experiment. As *Ri* was only used to classify stability and was not used in any calculations, we felt justified in using measurements from a Mesonet site to classify stability at the ARM site.

Stability thresholds were defined as follows:

Unstable: $Ri < 0$
Stable: $0 \leq Ri < 0.2$
Strongly Stable: $Ri \geq 0.2$

Unstable conditions were not divided into weakly and strongly unstable categories, as the majority of the multi-lidar measurements were collected during overnight, stable conditions and few data points were available during daytime, unstable conditions.

4.4. Variance Estimation

In order to mitigate the effects of random errors on variance calculations, Vickers and Mahrt [24] recommend averaging turbulent fluxes over a period of time that is longer than the local averaging time, T. In practical terms, T is the averaging time that is used to calculate wind speed deviations and represents the largest temporal scale of turbulence that is included in the variance calculation. In this work, turbulent fluctuations, u_i', were defined as the difference between the instantaneous wind speed, u_i, and the 10-min. mean wind speed, $\overline{u_i}$. The variance was then defined as the mean value of $u_i'^2$ over a 30-min. period. In addition, a linear detrending filter was applied to each hour-long data record prior to the calculation of variance to mitigate effects of nonstationarity.

5. RESULTS

5.1. Evaluation of Tri-Doppler Technique

The tri-Doppler technique was analyzed from 12 to 16 June 2013 between approximately 0000 and 1500 UTC (7 pm and 10 am local time) every day. (For the remainder of the day, the OU Streamline and Galion lidars were set to a vertical stare mode for a different objective of the experiment.)

First, data from the OU Streamline and Galion lidars were combined with a dual-Doppler technique to estimate mean wind speed and wind direction profiles. These profiles were compared to similar profiles from the WindCube lidar and the ARM Streamline lidar, which conducts a 3-min VAD scan every 15 minutes. Sample time-height cross-sections of the 1-min mean horizontal wind speed and wind direction from the dual-Doppler technique and the WindCube DBS scans

Wind Energ. 2015; **00**:1–16 © 2015 John Wiley & Sons, Ltd.
DOI: 10.1002/we
Prepared using weauth.cls

are compared to the 3-min averaged wind speed and wind direction from the ARM Streamline VAD scans in Fig. 3. The vertical resolutions of the dual-Doppler, WindCube, and ARM VAD wind profiles were 10 m, 20 m, and 26 m, respectively.

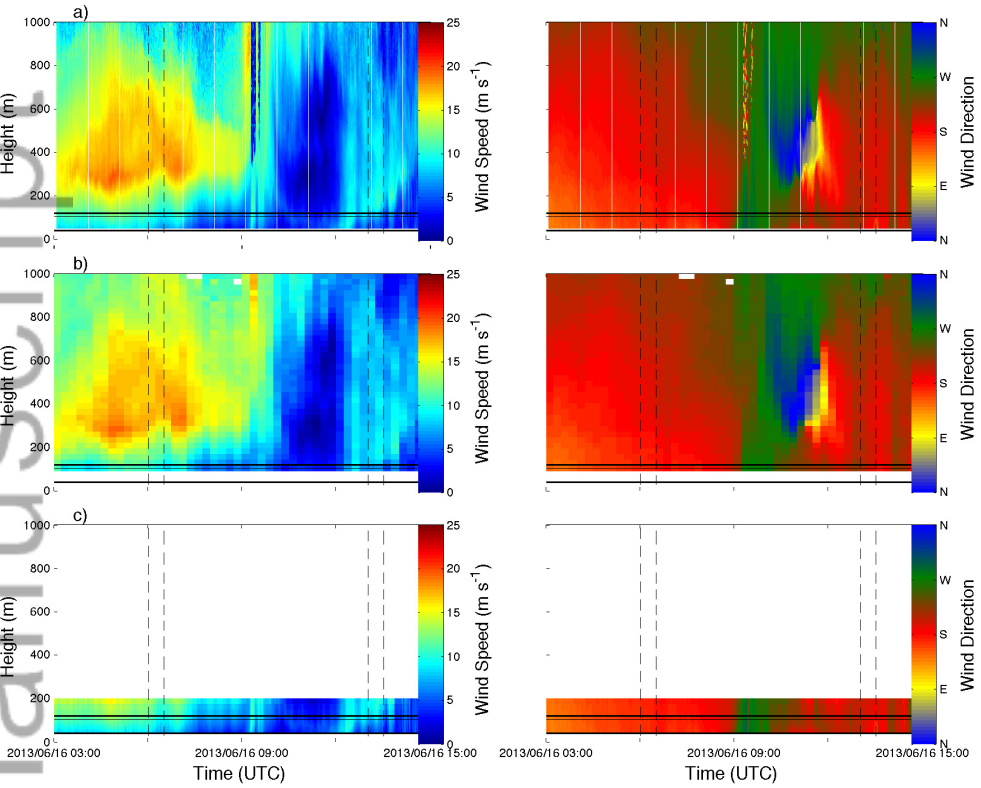

Figure 3. Time-height cross-sections of horizontal wind speed (left panels) and wind direction (right panels) derived from a) OU Streamline and Galion dual-Doppler technique b) ARM Streamline VAD scans and c) WindCube DBS scans on 16 June 2013. One-min means are shown in a) and c) and 15-min VAD values are shown in b). Thin black horizontal line denotes 105 m tri-Doppler analysis height and thick black lines denote the top and bottom of a typical turbine rotor disk in this area. (Note that maximum WindCube measurement height is 200 m.) Dashed lines indicate averaging periods for profiles shown in Fig. 4.

The difference in temporal and spatial resolution between the dual-Doppler technique and the ARM VAD scans is evident in Fig. 3, particularly in the development of a low-level jet (LLJ) from 0300 to 0900 UTC. Klein et al. [14] show a time-height cross-section from 13 June 2013, when undulations associated with atmospheric waves were observed in the dual-Doppler wind speed field but were not visible in the VAD fields. Features such as atmospheric waves and LLJs usually occur above the rotor disk area, but momentum and turbulence from these features can be transported downward and can impact power production and loads from a wind turbine [e.g., 25]. Thus, collecting measurements at heights above the turbine rotor disk is important for understanding boundary layer features that affect turbine performance. Although a vertically profiling WindCube lidar can take measurements at heights corresponding to a typical turbine rotor disk, it is unable to observe these mid- to upper-boundary layer features (Fig. 3c). The ability of a multi-lidar technique to collect high-resolution measurements above the turbine rotor disk is one major advantage over using a single vertically profiling lidar.

Despite the difference in temporal and vertical resolution in the wind speed and wind direction profiles evident in Fig. 3, profiles of 30-min mean values were quite similar for two 30-min time periods on the early morning of 16 June 2013 (Fig. 4) . In Fig. 4a, an LLJ core is visible around 450 m with a maximum wind speed of approximately 18 m s^{-1}. This LLJ core is located several hundred meters above a typical turbine hub height of 80 m, but strong speed shear associated with the LLJ is still evident in the heights corresponding to a typical rotor disk area. Strong speed shear across the rotor disk area is also evident in Fig. 4c; while the wind speed profile between 200 and 1000 m AGL has started to become more uniform as a result of daytime turbulent mixing, speed shear is still evident below 200 m AGL.

Overall, 30-min. mean wind speeds measured by the dual-Doppler technique were well-correlated to wind speeds measured by the WindCube lidar (R^2 = 1.00, N = 1832) and slightly less correlated to wind speeds measured by the VAD technique with the ARM lidar (R^2 = 0.81, N = 7726). Root-mean squared error (*RMSE*) and bias values were small

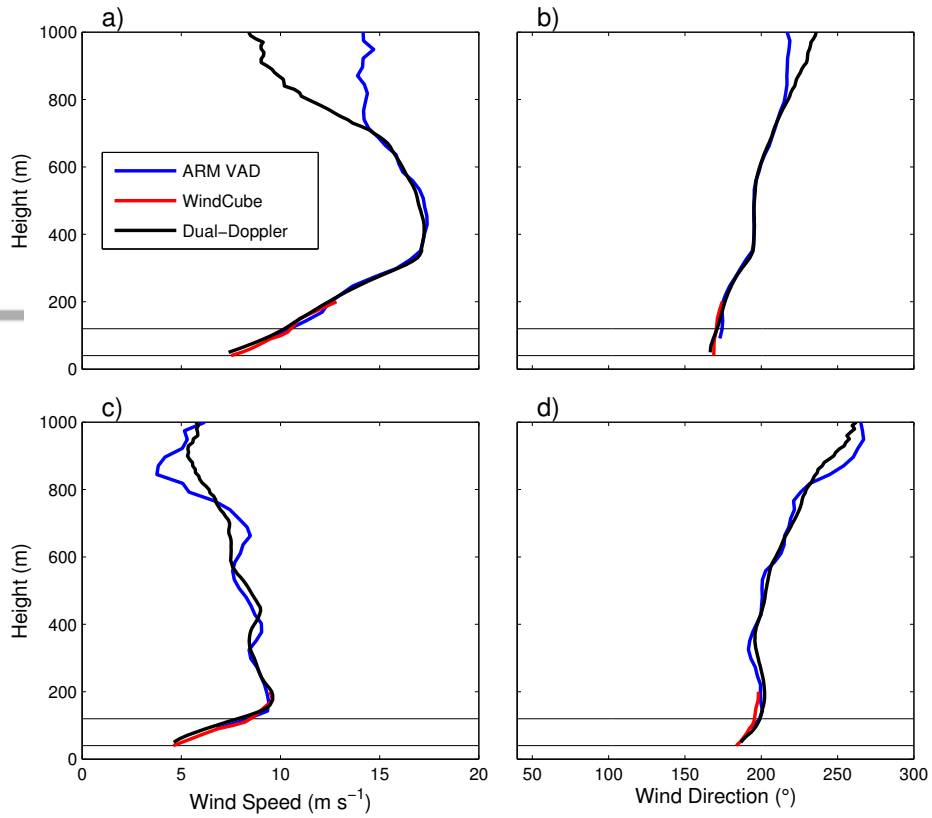

Figure 4. 30-min mean wind speed (a, c) and wind direction (b, d) profiles from 0600-0630 UTC (1:00-1:30 AM local time) (top panels) and 1300-1330 UTC (8:00-8:30 AM local time) (bottom panels) on 16 June 2013. Horizontal black lines denote the top and bottom of a typical turbine rotor disk in this area.

when the dual-Doppler estimates were compared to the WindCube estimates ($RMSE$ = 0.54 m s^{-1}, bias = 0.37 m s^{-1}) and larger for the VAD estimates ($RMSE$ = 5.40 m s^{-1}, bias = 0.49 m s^{-1}). The large RMSE value between the dual-Doppler and VAD estimates was likely caused by the temporal resolution of the scans; while the dual-Doppler technique obtained a new wind speed profile estimate every 1 min., the ARM lidar only obtained wind profile estimates every 15 min. with the VAD technique. One-min. averages of the wind speed measured by the dual-Doppler technique also agreed well with one-min. averages from the WindCube lidar (R^2 = 0.99, $RMSE$ = 0.75 m s^{-1}, bias = 0.36 m s^{-1}, N = 52594). Wind direction estimates from the dual-Doppler technique were also well-correlated to measurements from the WindCube and ARM lidar ($R^2 > 0.9$ for both datasets), while somewhat large bias and RMSE values indicated possible misalignment among the different instruments. However, this misalignment does not affect mean wind speed estimates or the rotated variance components discussed in this work.

Figure 5 shows mean wind speeds and wind directions measured at the analysis height of 105 m by the WindCube lidar and the tri-Doppler technique. The mean wind speeds and wind directions measured by the two different techniques correspond well to one another ($R^2 > 0.99$), despite the fact that the sampling volumes of the techniques were approximately 200 m apart (Fig. 2a). Thus, heterogeneity in the mean horizontal flow did not appear to be a large factor at the site.

Scatter plots of the 30-min variance values measured by the tri-Doppler and DBS (WindCube) techniques at 105 m and stratified by stability are shown in Fig. 6. The WindCube tended to measure higher u and v variance values than the tri-Doppler technique under unstable conditions (Figs. 6a, b), likely as a result of variance contamination, which is most prevalent during unstable periods [7]. Although results from the unstable cases are only based on a small number of 30-min periods, the same WindCube lidar used during LABLE 2 was significantly affected by variance contamination under unstable conditions during a similar experiment in Colorado [26].

In contrast, the tri-Doppler technique often measured higher v variance values than the WindCube lidar under stable conditions (Fig. 6b). As discussed later in the section, the tri-Doppler technique likely measured higher values of the v

Wind Energ. 2015; **00**:1–16 © 2015 John Wiley & Sons, Ltd.
DOI: 10.1002/we
Prepared using weauth.cls

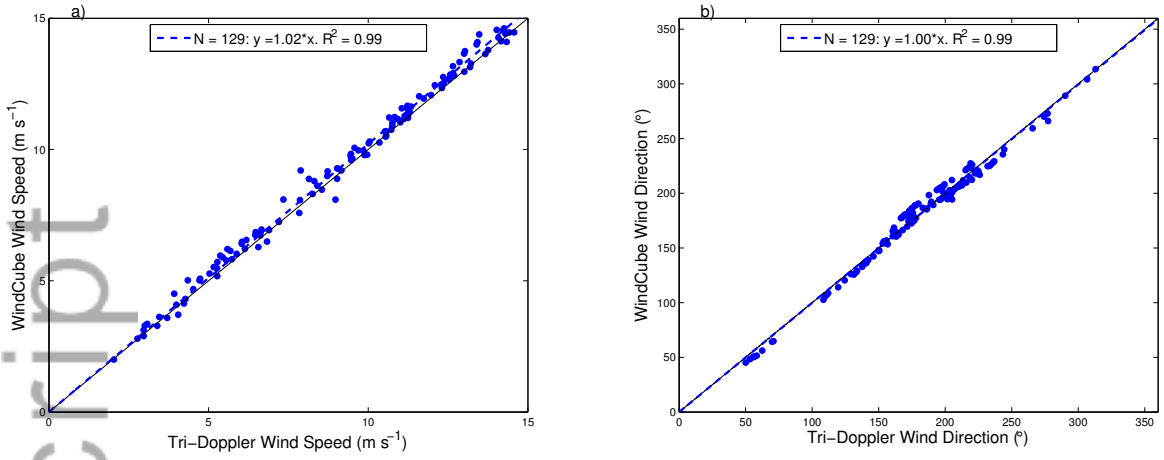

Figure 5. Scatter plots of 30-min mean a) wind speed and b) wind direction from WindCube lidar and tri-Doppler technique at 105 m AGL. One-to-one line is shown in black for reference and regression fits are indicated by blue dashed lines. In b), wind direction values that were less than 15° were added to 360° to avoid biasing the regression line for wind directions near northerly.

variance under stable conditions because it does not require averaging across a scanning circle and the technique can obtain independent velocity estimates at a higher frequency than the WindCube lidar.

Vertical variance measured using the DBS technique with the WindCube lidar was quite similar to variance measured by the tri-Doppler technique, with regression line slopes ranging from 0.86 to 1.1 (Fig. 6c). However, the WindCube lidar nearly always measured larger w variance values than the tri-Doppler technique when the vertically pointed beam was used to estimate the variance (Fig. 6d). With the standard WindCube DBS scanning strategy, the vertical variance is calculated from average values of w across the scanning circle. However, when the vertical beam is used to estimate variance, values of w are obtained from probe volumes directly above the lidar, resulting in larger WindCube vertical variance values when the vertical beam is used (Fig. 6d). As shown in [26], vertical variance measured by the WindCube's vertical beam is much closer to variance measured by a sonic anemometer, and thus is likely a better measure of the true variance. The difference between the WindCube and tri-Doppler vertical variance estimates in Fig. 6d is likely related to the difference in probe volume between the two techniques; the WindCube's probe volume length is 20 m, while the probe volume length of the scanning lidars was set to 30 m, which would serve to decrease the tri-Doppler-estimated variance in comparison to the WindCube as a result of volume averaging.

Averaged velocity spectra for strongly stable, stable, and unstable conditions are shown in Fig. 7. As the WindCube lidar only obtains independent velocity data every four seconds (i.e., the time it takes to complete a full scan), four-second data were used to calculate the spectra.

Under strongly stable and stable conditions, the WindCube and tri-Doppler u and v spectra agree quite well up until just before the 0.125 Hz cut-off, the Nyquist frequency of the independent WindCube data. The tri-Doppler spectra continue up until 0.5 Hz, as the tri-Doppler scans obtain independent data every 1 second and have a true Nyquist frequency of 0.5 Hz. The ability of the tri-Doppler technique to measure turbulence at these higher frequencies (between 0.125 and 0.5 Hz) likely led, in part, to the higher u and v variance values measured under stable conditions in comparison to the WindCube DBS technique (Figs. 6a, b). The lack of scanning circle averaging also likely contributed to the higher horizontal variance values measured by the tri-Doppler technique, although it is difficult to quantify this contribution without information on the spatial variability of turbulence at the site.

Some small differences in the v spectra under strongly stable conditions are evident in the top panel of Fig. 7b. Between frequencies of approximately 0.05 to 0.125 Hz, the WindCube spectral energy increases slightly and becomes higher than the tri-Doppler spectral energy. As this increase in spectral energy is located in the high-frequency range, it is likely associated with noise in the raw WindCube velocity data. This increase in spectral energy is reflected in the overestimation of v variance values by the WindCube lidar that frequently occurred under strongly stable conditions (Fig. 6b). Thus, the differing sensitivity and levels of instrument noise between the WindCube lidar and the scanning lidars likely affected the variance estimates in addition to the spatial and temporal resolution of the measurements.

Under unstable conditions, the WindCube u and v spectra have slightly higher energy than the tri-Doppler spectra for frequencies before the cut-off at 0.125 Hz (bottom panels in Fig. 7). Cañadillas et al. [27] found similar results when comparing averaged WindCube spectra to sonic anemometer spectra and attribute the increase in spectral energy to variance contamination. Although the tri-Doppler dataset was mainly limited to the overnight hours (stable conditions), the u and v variance values that were measured under unstable conditions by the tri-Doppler technique were nearly always lower than

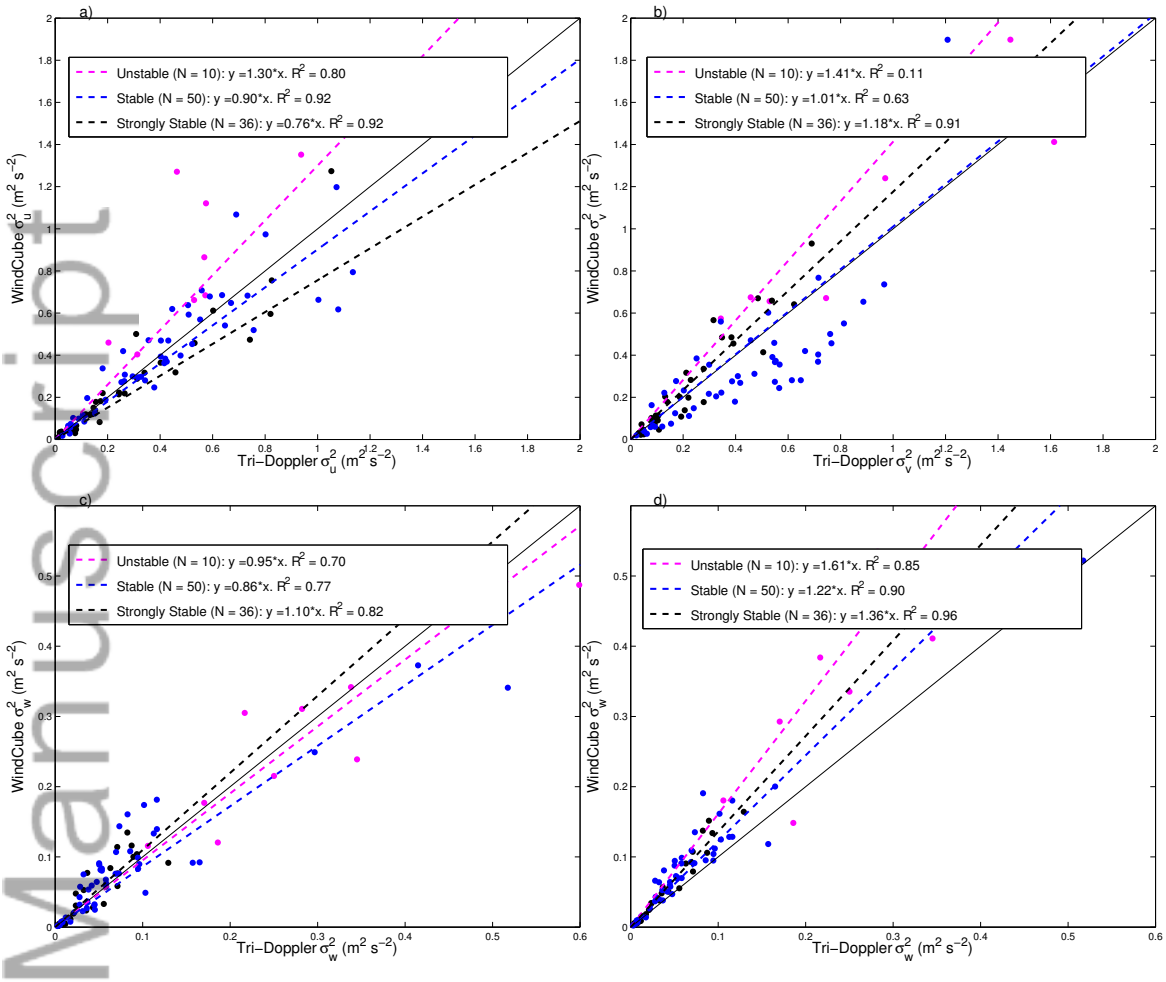

Figure 6. Scatter plots of 30-min tri-Doppler variance versus WindCube variance at 105 m AGL stratified by stability (circles) and regression lines for different stability classes (dashed lines). In all figures, one-to-one line is shown in black for reference. Scatter plots for a) *u* variance, b) *v* variance and c) and d) *w* variance are shown. In c), *w* variance from WindCube lidar is estimated from DBS technique and in d) it is estimated directly from the vertical beam position.

those measured by the WindCube lidar, reflecting the increase in WindCube variance caused by variance contamination (Figs. 6a, b).

For all three stability classes, the WindCube *w* spectra show higher spectral energy than the tri-Doppler spectra for nearly all frequencies (Fig. 7c). This suggests that the probe volume size (Δz = 20 m for the WindCube compared to Δz = 30 m for the scanning lidars) has a large effect on the measurement of vertical variance, although it is difficult to assess the impact of other factors, such as instrument noise and sensitivity.

5.2. Virtual Tower Technique

The virtual tower technique was evaluated at the ARM site from 28 June to 3 July. Unlike the tri-Doppler technique, the virtual tower technique allows for the measurement of turbulence at multiple heights such that the vertical profile of turbulence can be observed; however, these turbulence measurements are collected at the expense of the temporal resolution. In order to investigate the usefulness of virtual tower turbulence measurements, turbulence measured from the virtual tower technique was compared to 10-min variance values measured by the WindCube lidar for each hour. In this section, 10-min, rather than 30-min, variance values are shown, as the scanning lidar beams were pointed at each measurement height for 10 min.

A sample time series of the 10-min variance measured by the WindCube lidar at 100 m AGL is shown in Fig. 8. Two hour-long time periods were selected for further analysis: 0800 to 0900 UTC, which occurred under strongly stable conditions, and 1700 to 1800 UTC, which occurred under unstable conditions.

Wind Energ. 2015; **00**:1–16 © 2015 John Wiley & Sons, Ltd.
DOI: 10.1002/we
Prepared using weauth.cls

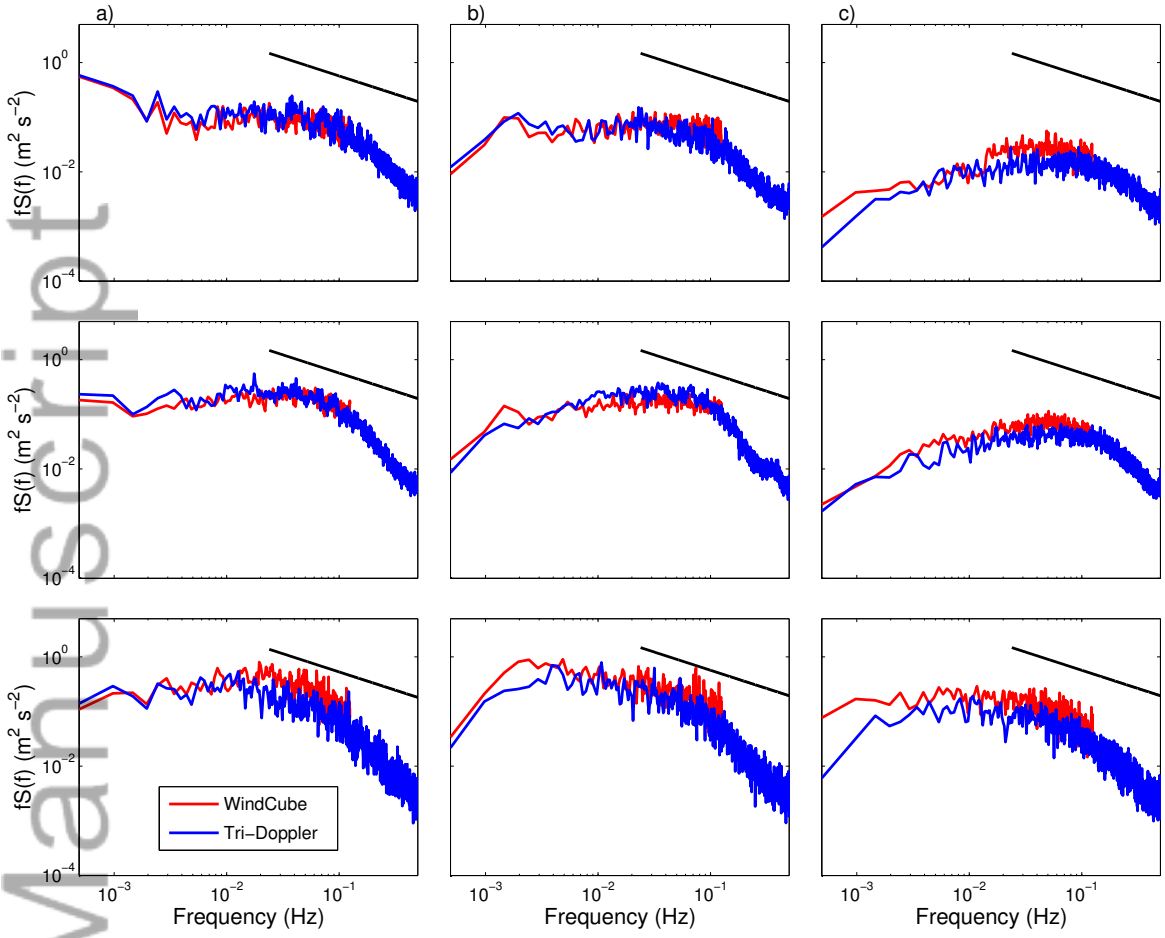

Figure 7. Average a) *u* velocity b) *v* velocity and c) *w* velocity spectra from tri-Doppler technique and WindCube lidar at 105 m AGL. Spectra from strongly stable (top), stable (middle), and unstable (bottom) atmospheric conditions are shown. Black solid line indicates -2/3 slope (inertial subrange). In a) and b), WindCube spectra were calculated using independent data obtained every four seconds. In c), WindCube spectra were calculated using only data from the vertical beam.

Variance and wind speed profiles measured by the various techniques from 0800 to 0900 UTC on 3 July 2013 (3:00 to 4:00 am local time) are shown in Fig. 9. Profiles measured by the WindCube lidar show the variance decreasing to a height of approximately 100 m before remaining relatively constant with height, then increasing from 120 to 200 m (Figs. 9a–c). The mean wind speed increases from 4 to 100 m before decreasing slightly, which could indicate an LLJ nose at 100 m (Fig. 9d). These profiles are similar to the composite LLJ profiles presented by Banta et al. [28], where the approximate minimum in variance is located at the height of the wind speed maximum. Large variance values measured by the WindCube lidar above the LLJ nose were likely associated with noisy data, as 200 m is the maximum measurement height of the WindCube lidar, and the signal-to-noise ratio of WindCube measurements is typically optimized at approximately 100 m AGL. However, it is difficult to determine whether the WindCube or virtual tower measurements of variance were more accurate at 200 m, as no in-situ data were available at 200 m.

Variance values measured by the virtual tower technique and the WindCube DBS technique were quite similar at 60 and 100 m AGL, with little variation indicated in the 10-min WindCube variance values throughout the hour-long period (Figs. 9a–c). The horizontal variance values measured by the WindCube lidar were larger than those measured by the virtual tower technique at 200 m, likely due to noise, as discussed in the previous paragraph. In general, however, the variance values measured by the virtual tower technique were similar to those measured by the WindCube lidar and were nearly always located within one standard deviation of the mean 10-min variance value measured by the WindCube lidar during the hour-long period. Mean wind speed profiles measured by the virtual tower technique were very close to those measured by the WindCube lidar (Fig. 9d).

A similar profile is shown in Fig. 10 for 1700 to 1800 UTC on 3 July 2013 (12:00 to 1:00 pm local time), which corresponded to unstable atmospheric conditions. Variance values measured during this time period were much larger than

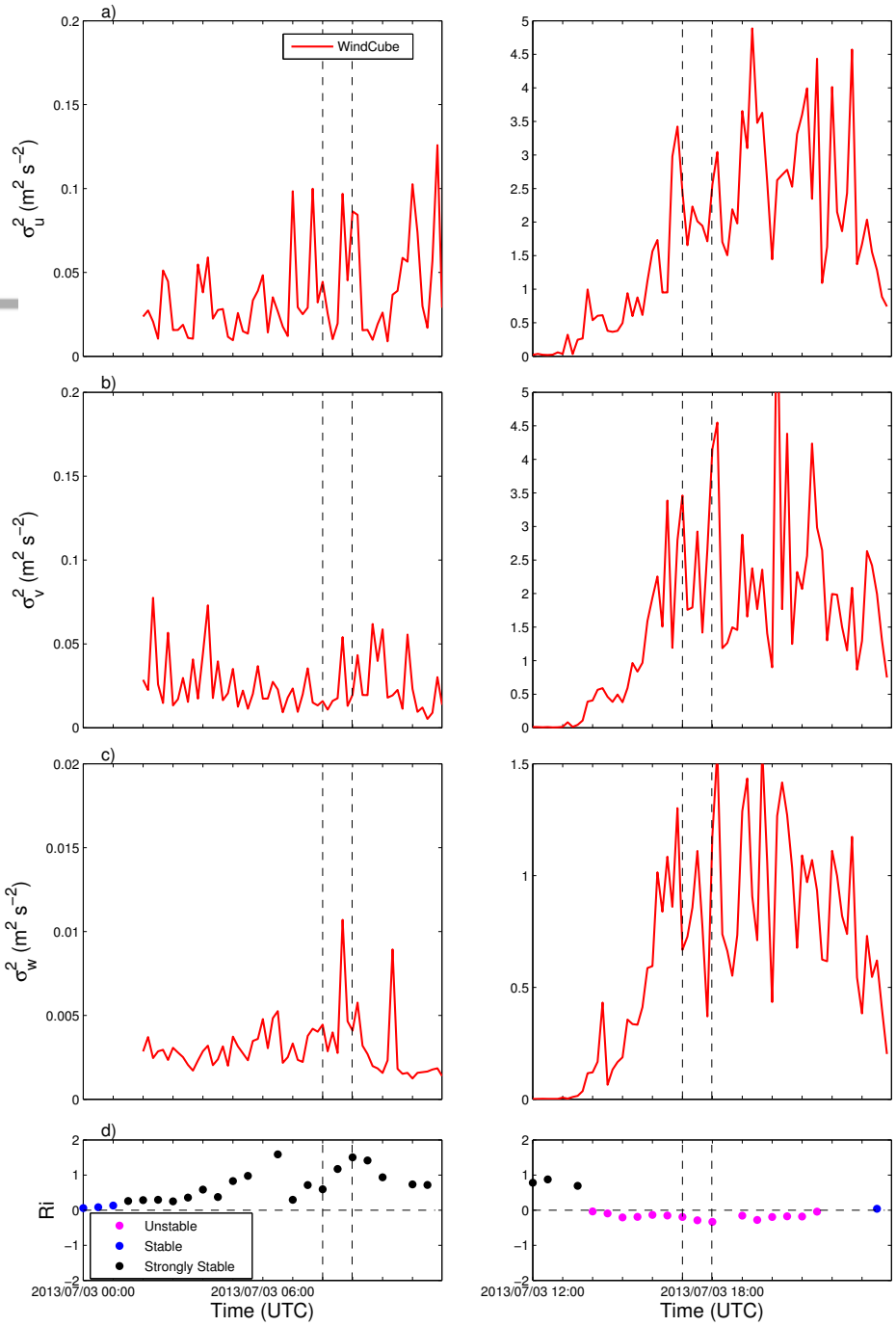

Figure 8. Time series of 10-min a) *u* b) *v* and c) *w* variance from WindCube lidar at 100 m AGL and d) *Ri* from Blackwell Mesonet site on 3 July 2013. Left panels show data from 0000 to 1200 UTC and right panels show data from 1200 to 2359 UTC (time series was split into two panels to better depict variance of different magnitudes). Vertical dashed lines in each figure enclose hour-long periods discussed later in the text.

those measured during the stable period in Fig. 9. In addition, the 10-min variance values changed fairly significantly over the course of the hour as the convective boundary layer developed (Figs. 8, 10). However, the mean variance profile did not change significantly with height, which is to be expected in the surface layer or "constant flux layer" according to

Wind Energ. 2015; **00**:1–16 © 2015 John Wiley & Sons, Ltd.
DOI: 10.1002/we
Prepared using weauth.cls

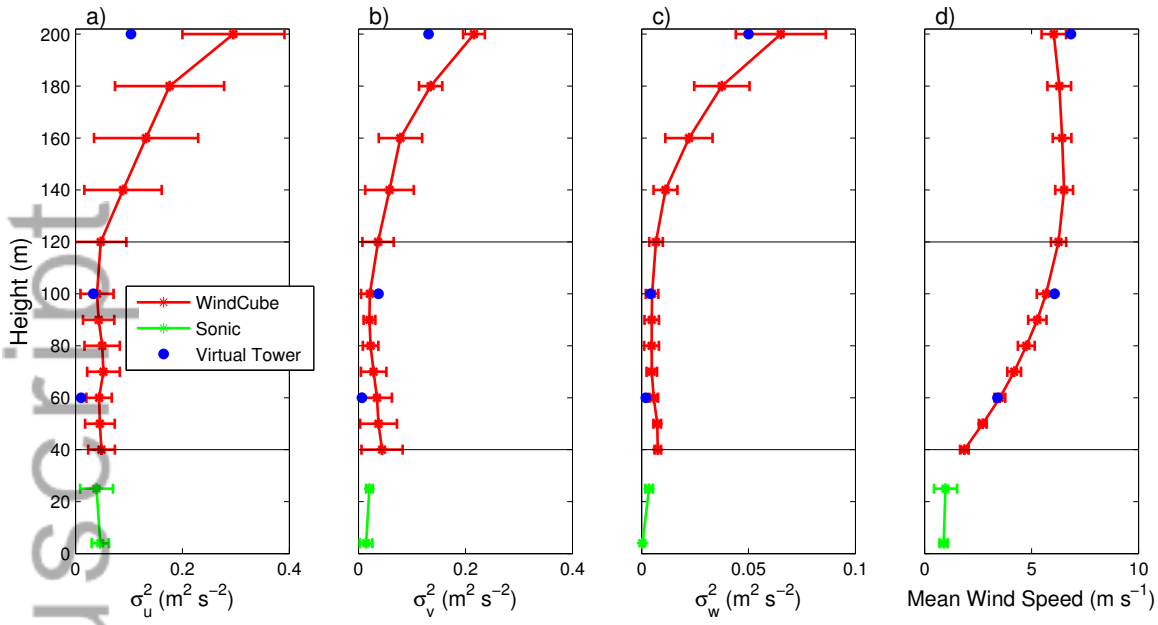

Figure 9. Profiles of a) *u* b) *v* and c) *w* variance and d) mean wind speed measured by virtual tower technique, WindCube lidar, and sonic anemometers at the ARM site on 3 July 2013 from 0800 to 0900 UTC (strongly stable conditions). Virtual tower markers show variance and mean wind speed calculated from the 10-min subsets of velocity data collected at each height, while WindCube and sonic anemometer circles and error bars indicate the mean and standard deviation of the 10-min variance values and mean wind speeds measured throughout the hour-long time period. Horizontal black lines denote the top and bottom of a typical turbine rotor disk in this area.

similarity theory [e.g., 29]. The wind speed profile is also uniform, in accordance with a well-mixed convective boundary layer (Fig. 10d).

During this period, the WindCube lidar nearly always measured larger horizontal variance values than the virtual tower technique. The larger *u* and *v* variance estimates are likely related to variance contamination [7]. Both the 4- and 25 -m sonic anemometers and the WindCube lidar measured a large variation in 10-min variance values throughout this hour-long time period, which was not captured by the virtual tower technique, as the virtual tower technique involves moving the lidars to a different measurement height every 10 min.

6. SUMMARY AND CONCLUSIONS

In this work, two different multi-lidar scanning strategies, the tri-Doppler technique and the virtual tower technique, were evaluated for their ability to measure low-level turbulence and mean wind speeds. Under stable conditions, the tri-Doppler technique tended to measure higher values of *u* and *v* variance in comparison to the WindCube lidar. Unlike the DBS technique used by the WindCube, the tri-Doppler technique allows for the accurate measurement of turbulent motions at frequencies up to 0.5 Hz and it does not involve averaging across a scanning circle. In contrast, the WindCube lidar produced larger estimates of the horizontal variance under unstable conditions, likely due to variance contamination. Both techniques measured vertical variance with a vertically pointing beam, which is not affected by variance contamination or scanning circle averaging. Differences in the vertical variance values measured by both techniques appear to be mainly related to the difference in probe volume size between the WindCube lidar and the scanning lidars.

In order to take turbulence measurements at multiple heights, a virtual tower technique was also implemented at the ARM site. The three scanning lidars pointed at several measurement heights directly above the WindCube lidar to estimate a variance profile. Under stable conditions, when variance was small and did not vary significantly with time, the virtual tower technique measured similar variance profiles to the WindCube lidar. However, under unstable conditions, the variance values changed significantly over the course of an hour and the virtual tower variance profiles did not fully represent the variance values experienced throughout the hour. In addition, the virtual tower technique appeared to measure lower horizontal variance values than the WindCube lidar under unstable conditions, likely due to variance contamination in the WindCube lidar data. Thus, while the virtual tower technique appears to be most well-suited for measuring turbulence

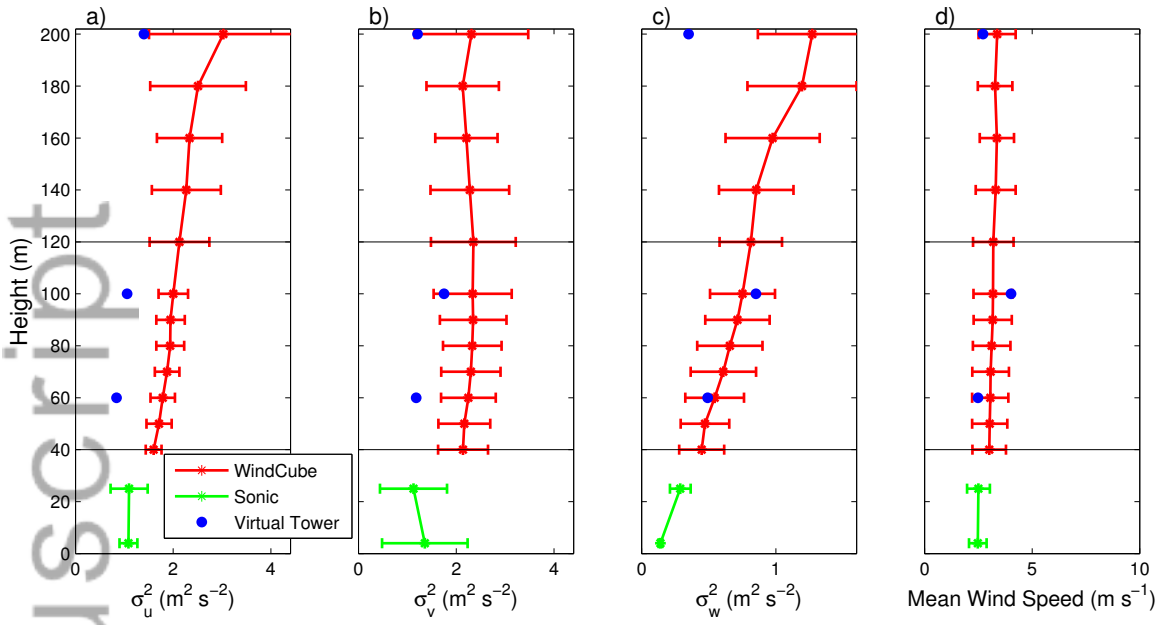

Figure 10. As in Fig. 9, but for 1700 to 1800 UTC (unstable conditions).

profiles under stable conditions, when variance does not change significantly with time, it also shows promise for reducing variance contamination under unstable conditions. Tall towers instrumented with sonic anemometers are needed to study the virtual tower technique in more detail, as all lidars are subject to measurement uncertainties and high-quality turbulence measurements are necessary to fully validate the technique.

While the tri-Doppler technique optimizes temporal resolution and the virtual tower technique optimizes spatial resolution, neither of these techniques is ideal for the measurement of turbulence, as turbulence can vary significantly in both time and space. However, more research is needed to determine if 3-D atmospheric turbulence measurements are important for wind energy applications. Results from a recent power curve modeling study demonstrated that the measurement of mean wind speeds across the turbine rotor disk improved power prediction, while the measurement of wind speed standard deviations across the entire rotor disk by a WindCube lidar did not provide significant improvements in power prediction over just using the hub-height value [30]. These results were only presented for one unwaked turbine in complex terrain in California, although a similar study is currently being conducted at a wind farm in flat terrain. The results suggest that the tri-Doppler technique, which only measures turbulence at one height, could provide sufficient inflow data for turbine power prediction. The tri-Doppler technique allows for the constant estimation of turbulence parameters at one height as well as estimation of mean wind speeds at several heights spanning a typical turbine rotor disk. In addition to turbine inflow conditions, the tri-Doppler technique could be used to study turbine wakes, as the technique does not require the assumption of horizontal flow homogeneity across a scanning circle.

In general, the tri-Doppler technique is much easier to implement than a virtual tower technique, as it does not require the exact temporal synchronization of scan angles from multiple lidars. Research on the performance of the tri-Doppler technique at a site with multiple sonic anemometers is currently ongoing [13] and should be supplemented by further research on the performance of the technique under different stability conditions and at sites in both flat and complex terrain.

6.1. Acknowledgements

The authors would like to thank the staff of the Southern Great Plains ARM site, Marc Fischer and Sebastien Biraud from Lawrence Berkeley National Laboratory, the members of the Boundary Layer Integrated Sensing and Simulation group at OU, and the technical support staff at Sgurr Energy, Leosphere, and Halo Photonics for their assistance during the experiment. We are also grateful for comments from two anonymous reviewers, which helped improve the manuscript. LABLE 2 data were obtained from the Atmospheric Radiation Measurement (ARM) Climate Research Facility, a U.S. Department of Energy Office of Science user facility sponsored by the Office of Biological and Environmental Research. JFN and SW received funding from Laboratory Directed Research and Development (LDRD) award number 12-ERD-069 from the Lawrence Livermore National Laboratory.

6.2. Bibliography

1. Schreck S, Lundquist J, Shaw W. U.S Department of Energy workshop report: Research needs for wind resource characterization. *Technical Report NREL/TP-500-43521*, National Renewable Energy Laboratory 2008.
2. Strauch RG, Merritt DA, Moran KP, Earnshaw KB, De Kamp DV. The Colorado wind-profiling network. *J. Atmos. Oceanic Technol.* 1984; **1**:37–49.
3. Browning KA, Wexler R. The determination of kinematic properties of a wind field using Doppler radar. *J. Appl. Meteor.* 1968; **7**:105–113.
4. Bingöl F, Mann J, Foussekis D. Conically scanning lidar error in complex terrain. *Meteor. Z.* 2009; **18**:189–195.
5. Lundquist JK, Churchfield MJ, Lee S, Clifton A. Quantifying error of lidar and sodar Doppler beam swinging measurements of wind turbine wakes using computational fluid dynamics. *Atmos. Meas. Tech.* 2015; **8**:907–920.
6. Wainwright CE, Stepanian PM, Chilson PB, Palmer RD, Fedorovich E, Gibbs JA. A time series sodar simulator based on large-eddy simulation. *J. Atmos. Oceanic Technol.* 2014; **31**:876–889.
7. Sathe A, Mann J, Gottschall J, Courtney MS. Can wind lidars measure turbulence? *J. Atmos. Oceanic Technol.* 2011; **28**:853–868.
8. Newsom R, Calhoun R, Ligon D, Allwine J. Linearly organized turbulence structures observed over a suburban area by dual-Doppler lidar. *Bound.-Layer Meteor.* 2008; **127**:111–130.
9. Mann J, Cariou JP, Courtney MS, Parmentier R, Mikkelsen T, Wagner R, Lindelöw P, Sjöholm M, Enevoldsen K. Comparison of 3D turbulence measurements using three staring wind lidars and a sonic anemometer. *IOP Conference Series: Earth and Environmental Science* 2008; **1**:012 012.
10. Calhoun R, Heap R, Princevac M, Sommer J, Fernando H, Ligon D. Measurement of winds flowing toward an urban area using coherent Doppler lidar. *Fifth Conf. on the Urban Environment*, Amer. Meteor. Soc.: Vancouver, B. C., Canada, 2004; CD–ROM, 3.8.
11. Calhoun R, Heap R, Princevac M, Newsom R, Fernando H, Ligon D. Virtual towers using coherent Doppler lidar during the Joint Urban 2003 Dispersion Experiment. *J. Appl. Meteor.* 2006; **45**:1116–1126.
12. Newsom RK, Berg LK, Shaw WJ, Fischer ML. Turbine-scale wind field measurements using dual-Doppler lidar. *Wind Energy* 2015; **18**:219–235.
13. Fuertes FC, Iungo GV, Porté-Agel F. 3D turbulence measurements using three synchronous wind lidars: Validation against sonic anemometry. *J. Atmos. Oceanic Technol.* 2014; **31**:1549–1556.
14. Klein P, Bonin TA, Newman JF, Turner DD, Chilson PB, Wainwright CE, Blumberg WG, Mishra S, Carney M, Jacobsen EP, *et al.*. LABLE: A multi-institutional, student-led, atmospheric boundary-layer experiment. *Bull. Amer. Meteor. Soc.* 2015; **96**:1743–1764.
15. Bonin TA, Blumberg WG, Klein PM, Chilson PB. Thermodynamic and turbulence characteristics of the Southern Great Plains nocturnal boundary layer under differing turbulent regimes. *Bound.-Layer Meteor.* 2015; **157**:401–420.
16. Pearson G, Davies F, Collier C. An analysis of the performance of the UFAM pulsed Doppler lidar for observing the boundary layer. *J. Atmos. Oceanic Technol.* 2014/04/22 2009; **26**:240–250.
17. Fischer ML. Carbon dioxide flux measurement systems (CO_2FLX) handbook January 2004. URL http://www.arm.gov/publications/tech_reports/handbooks/co2flx_handbook.pdf.
18. Cariou JP, Boquet M. LEOSPHERE Pulsed Lidar Principles. Contribution to UpWind WP6 on Remote Sensing Devices. 2010. URL http://www.upwind.eu/Publications/~/media/UpWind/Documents/Publications/6%20-%20Remote%20Sensing/D611.ashx.
19. Sathe A, Mann J. Measurement of turbulence spectra using scanning pulsed wind lidars. *J. Geophys. Res.: Atmospheres* 2012; **117**:D01 201.
20. Kaimal J, Finnigan J. *Atmospheric Boundary Layer Flows: Their Structure and Measurement*. Oxford University Press, 289 pp., 1994.
21. McPherson RA, Coauthors. Statewide monitoring of the mesoscale environment: A technical update on the Oklahoma Mesonet. *J. Atmos. Oceanic Technol.* 2007; **24**:301–321.

22. Bodine D, Klein PM, Arms SC, Shapiro A. Variability of surface air temperature over gently sloped terrain. *J. Appl. Meteor. Climatol.* 2009; **48**:1117–1141.

23. Newman JF, Klein PM. The impacts of atmospheric stability on the accuracy of wind speed extrapolation methods. *Resources* 2014; **3**:81–105.

24. Vickers D, Mahrt L. Quality control and flux sampling problems for tower and aircraft data. *J. Atmos. Oceanic Technol.* 1997; **14**:512–526.

25. Kelley ND, Shirazi M, Jager D, Wilde S, Adams J, Buhl M, Sullivan P, Patton E. Lamar low-level jet project interim report. *Technical Report NREL/TP-500-34593*, National Renewable Energy Laboratory 2004.

26. Newman JF, Klein PM, Wharton S, Sathe A, Bonin TA, Chilson PB, Muschinski A. Evaluation of three lidar scanning strategies for turbulence measurements. *Atmos. Meas. Tech. Discuss.* 2015; **8**:12 329–12 381.

27. Cañadillas B, Westerhellweg A, Neumann T. Testing the performance of ground-based wind LiDAR system. *DEWI Magazine* 2011; (38):58–64.

28. Banta RM, Pichugina YL, Brewer WA. Turbulent velocity-variance profiles in the stable boundary layer generated by a nocturnal low-level jet. *J. Atmos. Sci.* 2006; **63**:2700–2719.

29. Arya SP. *Introduction to Micrometeorology*, *International Geophysics Series*, vol. 79. 2nd edn., Academic Press: Cornwall, UK, 2001.

30. Bulaevskaya V, Wharton S, Clifton A, Qualley G, Miller WO. Wind power curve modeling in complex terrain using statistical models. *Journal of Renewable and Sustainable Energy* 2015; **7**:013 103.

7. COPYRIGHT STATEMENT

Please be aware that the use of this LaTeX 2ε class file is governed by the following conditions.

7.1. Copyright

ACKNOWLEDGEMENT

This class file was developed by Sunrise Setting Ltd, Torquay, Devon, UK. Website:
www.sunrise-setting.co.uk